Effect of Molecular Architecture on Dynamics of Multigraft Copolymers: Combs, Centipedes, and Barbwires

Jovan Mijović* and Mingyun Sun

Othmer Department of Chemical and Biological Sciences and Engineering and The Herman F. Mark Polymer Research Institute, Polytechnic University, Six MetroTech Center, Brooklyn, New York 11201

Srdjan Pejanović

Department of Chemical Engineering, Faculty of Technology, University of Belgrade, Karnegijeva 4, Belgrade, 11000 Serbia and Montenegro

Jimmy W. Mays

Department of Chemistry, University of Tennessee, 655 Buehler Hall, Knoxville, Tennessee 37996

Received June 27, 2003; Revised Manuscript Received August 7, 2003

ABSTRACT: An investigation was carried out on the effect of molecular architecture on the dynamics of multigraft (MG) copolymers of polyisoprene (PI) and polystyrene (PS). MG copolymers with regularly spaced multiple grafts with trifunctional (combs), tetrafunctional (centipedes), and hexafunctional (barbwires) branch points were synthesized by anionic polymerization and studied by dielectric relaxation spectroscopy (DRS) and dynamic mechanical spectroscopy (DMS). The PI precursors were characterized by the presence of segmental and normal mode processes. The temperature dependence of the dielectric relaxation time for the segmental (τ_S) and normal mode (τ_N) process was of the Vogel−Fulcher−Tammann (VFT) type. In the entangled regime τ_N scales with $M^{4.0}$. The major findings for the MG copolymers are as follows: (1) all MG copolymers are characterized by the presence of segmental and normal mode relaxation; (2) τ_S is independent of molecular weight and architecture; (3) τ_N is slower in a MG copolymer than in its PI precursor; (4) τ_N in a MG copolymer of a given architecture is not a function of the overall molecular weight or the number of branch points; (5) the difference between the normal mode relaxation time for a MG copolymer, $\tau_{N(PIPS)}$, and its PI precursor, $\tau_{N(PI)}$, defined as $\Delta\tau_N = \tau_{N(PIPS)} - \tau_{N(PI)}$, depends strongly on the molecular weight of the PS graft (M_{PS}). An explanation was offered for the reasons underlying the observed slowdown of the normal mode relaxation in MG copolymers vis-à-vis their PI precursors.

Introduction

Strong experimental, theoretical, and computational efforts are currently underway aimed at understanding how molecular architecture affects dynamics in an array of complex systems based on synthetic and/or biological macromolecules.[1] The work reported herein addresses this issue for a series of multigraft (MG) copolymers with polyisoprene (PI) backbone and polystyrene (PS) grafts. The MG copolymers studied have regularly spaced multifunctional branch points and are synthesized in the form of combs, centipedes, and barbwires. A schematic representation of the three architectures investigated is shown in Figure 1. Although three branch points are depicted for the specimens in Figure 1, in practice the number of branch points may be varied.

In this work, dynamics were studied by dielectric relaxation spectroscopy (DRS) and dynamic mechanical spectroscopy (DMS). The presence of the PI block brings an added dimension to the study of dynamics by DRS; PI exhibits, in addition to the transverse dipole moment component ($\mu^{\perp}$) that gives rise to the segmental (α) process, a persistent cumulative dipole moment along the chain contour ($\mu^{\parallel}$).[2−20] This part of the dipole moment can be relaxed via the normal mode process (α_N). The term "normal mode" has found a widespread use in the polymer dynamics community to describe the *dielectric* relaxation due to the global motion of type A chains and is used here in that context. We acknowledge that Watanabe has strongly advocated the use of a fundamentally more correct term "eigenmode" in lieu of "normal mode" for the relaxation of mathematically well-defined modes.[13]

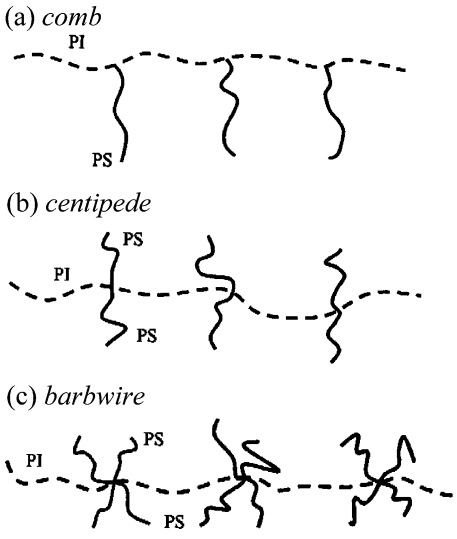

Figure 1. Molecular architecture of the regularly spaced multigraft (MG) poly(isoprene-*graft*-styrene) copolymers investigated: (a) combs, (b) centipedes, (c) barbwires. Dashed lines, PI backbone; solid lines, PS grafts.

* To whom correspondence should be addressed: e-mail jmijovic@poly.edu.

10.1021/ma034881g CCC: $25.00
Published on Web 09/11/2003

Table 1. Molecular Characteristics of PI Precursors and MG Copolymers.

sample code	M_{PS} (kg/mol)	no. of PS grafts/ branch point	M_{PI} (kg/mol)	unit M_u (kg/mol)	MG copolymers		no. of branch points
					M_u (kg/mol)	% PS	
PI1			34.2	34.2			
comb1-a					421	65.4	3.5
comb1-b	77.3	1	34.2	112	338	67.2	2.7
comb1-c					268	67.8	2.1
PI3			86.0	86.0			
comb2-a					515	18.4	3.7
comb2-b	31.6	1	86.0	118	391	19.0	2.6
comb2-c					315	19.0	2.0
PI4			87.6	87.6			
centipede-a					891	24.9	6.6
centipede-b	16.8	2	87.6	121	624	24.7	4.4
centipede-c					472	24.5	2.2
PI2			63.3	63.3			
barbwire-a					409	38.3	3.0
barbwire-b	13	4	63.3	115	328	37.9	2.3
barbwire-c					287	38.2	1.9

Chain molecules with a dipole moment parallel to the chain contour were termed type A by Stockmayer in his pioneering research on this subject.[14−17] An added attractive feature of those molecules is that, for a sequence of type A repeat units (without reversal of directional sense), the dipole vector must correlate with the displacement vector, implying a correspondence between dielectric and viscoelastic relaxations. The information obtained from those two techniques is complementary and hence conducive to an enhanced understanding of polymer dynamics. There are several excellent reviews in the literature that discuss the dynamics of type A polymers.[13,21]

To the best of our knowledge, this work is the first systematic study of segmental and normal mode dynamics of MG combs, centipedes, and barbwires. Several groups have been actively engaged in studying the effect of molecular architecture on the dynamics of linear diblock and triblock copolymers,[22−32] star copolymers,[26,33] and homopolymer/copolymer blends[34−36] as studied by dielectric techniques. We shall omit reviewing their work here; however, we shall contrast their findings with ours at appropriate places throughout the text.

The aim of the present work is to gain an insight into the nature of segmental and normal mode relaxation in MG copolymers of different component ratio, molecular weight, and molecular architecture.

Experimental Section

Materials. Polyisoprene (PI) and multigraft (MG) poly(isoprene-*graft*-styrene) copolymers were synthesized by anionic polymerization as described in detail elsewhere.[37] The two active macromolecular precursors, PI and PS, were prepared using bifunctional and monofunctional initiator, respectively. PI with a high 1,4 cis content was prepared using a lithium counterion in hydrocarbon media. PI used in this study is a typical type A polymer with noninverted dipole moment component parallel to the chain contour. Four different PIs were synthesized and labeled PI1, PI2, PI3, and PI4 in the order of increasing molecular weight (see Table 1). In the molecular weight range from 34 200 to 87 600 g/mol our PIs are in the entangled regime. Regularly spaced multigraft (MG) poly(isoprene-*graft*-styrene) copolymers were built into different architectures from the PI and PS precursors by controlling the functionality of chlorosilanes and producing chains with tri-, tetra-, or hexafunctional branch points shown in Figure 1.

A large number of samples were investigated, and frequent references to Table 1 will be necessary. The sample code adopted in the text for MG copolymers is simple: the samples are defined by their architecture, i.e., *comb*, *centipede*, and *barbwire*, and are written in italics. The two combs of different molecular weight are designated as *comb1* and *comb2*, in the order of increasing molecular weight of the PI block. Whenever necessary, a letter (*a*, *b*, or *c*) is appended to the sample name to denote a particular molecular weight fraction for a given architecture. The PI precursors are designated as PI1, PI2, PI3, and PI4, in the order of increasing molecular weight. All sample codes and pertinent information for PS and PI homopolymers and MG copolymers are summarized in Table 1. The number of branch points was calculated by subtracting the molecular weight of one PI chain (M_{PI}) from the overall molecular weight (M) of the MG copolymer and dividing by the molecular weight of the repeating unit of one PI spacer and PS grafts (M_u).

Techniques. *Dielectric Relaxation Spectroscopy* (*DRS*). Our facility combines commercial and custom-made instruments. A Novocontrol α high-resolution dielectric analyzer (3 μHz−10 MHz) and a Hewlett-Packard 4291 RF impedance analyzer were used. The instruments are interfaced to computers and equipped with heating/cooling controls, including a Novocontrol Novocool system custom-modified for sequential low- and high-frequency measurements. Further details of our DRS facility are given elsewhere.[38,39]

Dynamic Mechanical Spectroscopy (*DMS*). Experiments were conducted using a Rheometrics Scientific Advanced Rheometric Expansion System (ARES) rheometer. Measurements were performed in the frequency range from 0.01 to 100 rad/s and the temperature range from 213 to 323 K. A parallel plate configuration (plate diameter = 4 mm) was employed with a typical gap between the plates of ca. 1.0−2.0 mm. Strain values were adjusted from 0.01 to 0.1 for a measurable torque in the linear viscoelastic range, and linearity was verified by strain sweeps.

Differential Scanning Calorimetry (*DSC*). Glass transition temperatures were determined by DSC. The samples were first cooled at 20 K/min and then heated at 10 K/min. A TA Instruments Co. DSC model 2920 was used. The T_g was taken as the inflection point in the endothermic step in the heating trace.

Results and Discussion

Polyisoprene (PI) Precursors. We begin by examining the dielectric response of the four polyisoprene (PI) precursors used in this study whose molecular weights are listed in Table 1. Since DRS and DMS studies of neat PIs have been reported by several groups,[40−50] our goal here is not to be comprehensive. Nonetheless, we shall recap our findings and present some novel information for the PI precursors as the necessary prerequisite for the discussion of the dynamics of MG copolymers. DRS[2,51] results are presented first: dielectric permittivity and loss in the frequency domain with

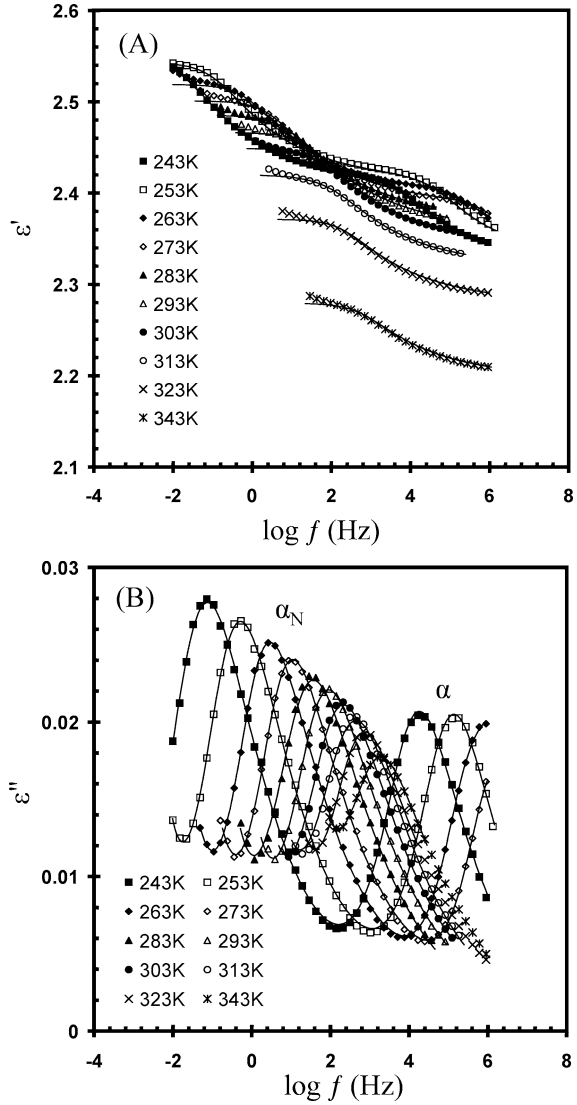

Figure 2. Dielectric permittivity (A) and loss (B) for PI1 (MW = 34 200 g/mol) in the frequency domain with temperature as a variable.

temperature as a variable are shown in parts A and B of Figure 2, respectively, for PI1 (M_{PI} = 34 200 g/mol, Table 1). Note how both modes, normal (α_N: lower frequency, Figure 2B) and segmental (α: higher frequency, Figure 2B), are beautifully discerned in the loss spectra. Analogous results were obtained for the higher molecular weight PI precursors, though we could not always capture both modes in a single frequency sweep at a fixed temperature because the gap between them increases with increasing molecular weight. In such cases we have evaluated normal and segmental modes in separate sweeps, focusing on the temperature range where each process is readily observable in our frequency window. The solid lines in Figure 2 are combined fits to two Havriliak−Negami (HN) functional forms,[52] for normal and segmental modes. The best results for the normal mode were obtained by setting the HN parameter $a = 1$, which reduces the HN equation to the Cole−Davidson (CD) equation.[53] The shape of the normal mode spectrum is independent of temperature for PI4 and is best described by the CD parameter $b = 0.26 \pm 0.01$. The characteristic change in the slope of the high-frequency end of the normal mode spectrum[21,29] was barely noticeable and only in the high molecular weight samples. This made fits to the CD equation

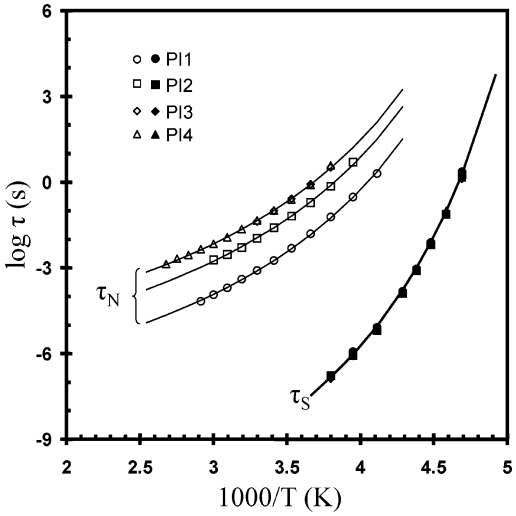

Figure 3. Temperature dependence of the average relaxation time for normal mode (τ_N: open symbols) and segmental mode (τ_S: solid symbols) with molecular weight as a parameter.

possible, though the character of these fits remains purely empirical. The calculated value of the Kohlrausch−Williams−Watts[54] β parameter (β_{KWW}) was equal to 0.45. This value is somewhat lower than the value reported by Boese and Kremer;[42] they found the β_{KWW} parameter to decrease with decreasing temperature from 0.6 to 0.54. Others, however, reported no effect of temperature on the spectral shape. For example, Floudas et al.[46] investigated the effect of temperature and pressure on the PI dynamics and found no effect on the shape parameters for the normal and segmental mode spectra. Adachi[43] also reported that the shape of the dielectric loss spectrum for normal and segmental modes was independent of temperature in the vicinity of glass transition. The segmental process is also thermodielectrically simple and is characterized by a Kohlrausch−Williams−Watts[54] β parameter (β_{KWW}) of 0.41. This result agrees with the data of Boese and Kremer,[42] who reported a β_{KWW} value of 0.40 ± 0.2 over a wide temperature range for PI of lower molecular weight (M_{PI} = 17 000 g/mol).

The temperature dependence of the relaxation time for normal (τ_N) and segmental (τ_S) mode in the neat PIs was examined next, and these results are plotted in Figure 3. Individual relaxation times were calculated using the τ_{HN} value and the following equation:

$$\tau_{max} = \tau_{HN}\left[\frac{\sin\left(\frac{\pi(1-a)b}{2(b+1)}\right)}{\sin\left(\frac{\pi(1-a)}{2(b+1)}\right)}\right]^{1/(1-a)} \quad (1)$$

where τ_{max} represents τ_N or τ_S, and a and b are the parameters in the HN equation. An increase in the molecular weight slows down the normal mode but has no effect on the segmental mode. We note that for linear PIs without dipole inversion we measure the longest relaxation time $\tau_N = \tau_1$ and stress that the calculated values of τ_{max} were practically identical to the corresponding values of τ_{ave} obtained directly from the data as $\tau_{ave} = {}^1/_2\pi f_{max}$. The solid lines in Figure 3 are best fits to the Vogel−Fulcher−Tammann (VFT) equation; the corresponding VFT parameters are displayed in Table 2. Note that excellent fits of the segmental process were obtained with the value of τ_{S0} fixed at the attempt

Table 2. VFT Parameters of Segmental and Normal Modes for MG Copolymers and PI Precursors

dynamic modes	M_{PI} (kg/mol)	M_{PS} (kg/mol)	no. of PS grafts/ branch point	VFT parameters		
				τ_0 (s)	B (K)	T_v (K)
segmental mode				1.0×10^{-14}	1662	162.5
normal mode						
PI1	34			1.1×10^{-6}	1498	162.5
PI2	63			1.7×10^{-8}	1507	162.5
PI3 and PI4	87			2.6×10^{-7}	1501	162.5
comb1	34	77	1	2.0×10^{-8}	2631	162.5
comb2	87	32	1	2.8×10^{-8}	2541	162.5
centipede	87	17	2	4.4×10^{-7}	2400	162.5
barbwire	63	13	4	1.1×10^{-7}	2377	162.5

frequency of 10^{-14} s, while the value of τ_{N0} of normal process varied as a function of molecular weight. Interestingly, excellent VFT fits for the normal mode process were obtained by setting the Vogel temperature (T_v) equal to the value obtained for the α process.

Next, we consider the molecular weight dependence of the spectral shape for normal and segmental modes. Recall that the spectral shape for the segmental process is independent of molecular weight and described by a single $\beta_{KWW} = 0.41$. The spectral shape for the normal mode was also independent of molecular weight except for PI1. Normalized loss spectra of that sample overlap tightly on the lower frequency side but are a bit broader on the high-frequency end in comparison with other PI precursors. This phenomenon is not caused by the encroachment with the segmental process (the two processes are ca. 5.3 decades apart) and is most likely due to the somewhat greater polydispersity (PDI = 1.29) of that sample.[37] The dianionic initiator used in synthesis of the PI segments gives higher polydispersity at low molecular weights. A similar effect of polydispersity on the spectral shape has been reported earlier.[40]

The results of dynamic mechanical spectroscopy (DMS) are examined next. Master curves of storage modulus (G') and loss modulus (G'') in the frequency domain for PI precursors with three different molecular weights at a reference temperature of 273 K are shown in parts A and B of Figure 4. The terminal and segmental relaxation time were calculated directly from the loss peak value $\tau = {}^1/_2\pi f_{max}$. In Figure 4, an additional small horizontal shift was applied to the master curves in order to coalesce the data in the segmental range and to bring out more clearly the molecular weight dependence in the terminal zone. Analogous to the DRS results, we find that increasing molecular weight slows down the terminal mode but has no effect on the segmental mode. The plateau modulus (G_N) was determined from Figure 4A by taking the value of the onset of transition from segmental to terminal mode. The thus obtained value of 3.5×10^5 Pa is in agreement with the result of Santangelo and Roland.[45] The calculated molecular weight between entanglements, M_e, of 6400 g/mol is in excellent agreement with the results of Santangelo and Roland[45] and Gotro and Graessley,[55] while somewhat higher than the value of 5400 g/mol reported by Floudas et al.[46] The critical molecular weight, M_c, of PI is about 10 000 g/mol.[40,42] Therefore, all PIs investigated in this work are in the entangled regime.

The molecular weight dependence of the normal mode relaxation time (τ_N) obtained from DRS is characterized by exponent 4.0 over a wide temperature range, as shown in Figure 5. Data reported by various investigators[40,42−43] are plotted together with our data in Figure 6, and the good agreement between the various results is apparent. Below the critical molecular weight (M_c = 10 000 g/mol), τ_N scales with $M^{2.0}$; above M_c, τ_N for our samples scales with $M^{4.0}$. The terminal relaxation time for all PIs obtained by DMS is also included in Figure 6, and the following findings are noted: (1) a good agreement between DRS and DMS data and (2) a good agreement between our data and the literature for the normal mode of PI above M_c. The relaxation time for the segmental mode (τ_S) of the PI precursors obtained from DMS measurements is also shown at the bottom

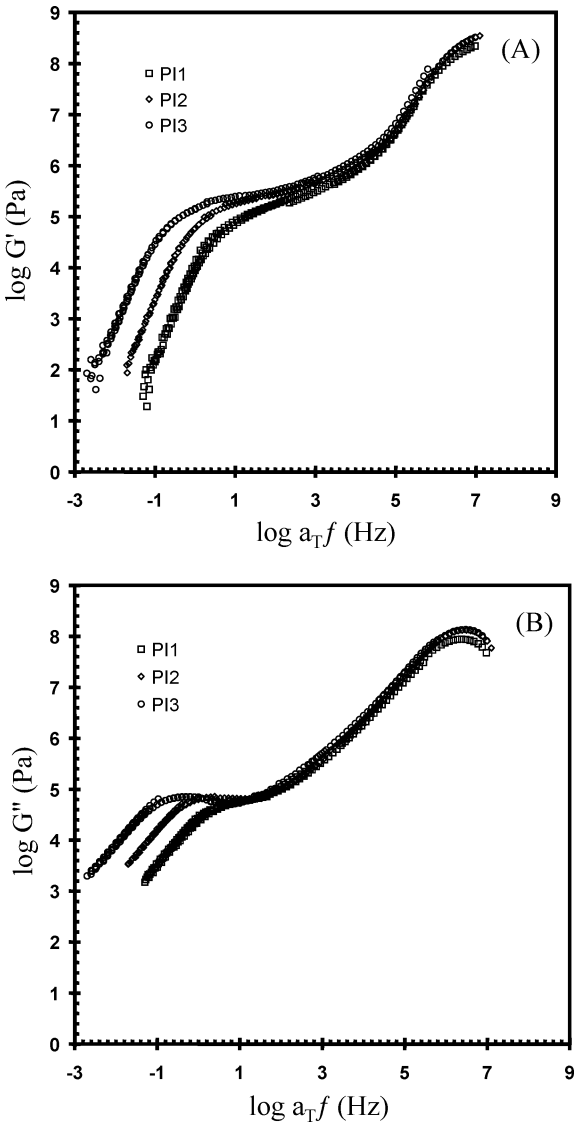

Figure 4. Master curves for storage modulus (A) and loss modulus (B) in the frequency domain for the four PI precursors at 273 K. Note that the segmental process is independent of molecular weight while the terminal process shifts to lower frequency with increasing molecular weight.

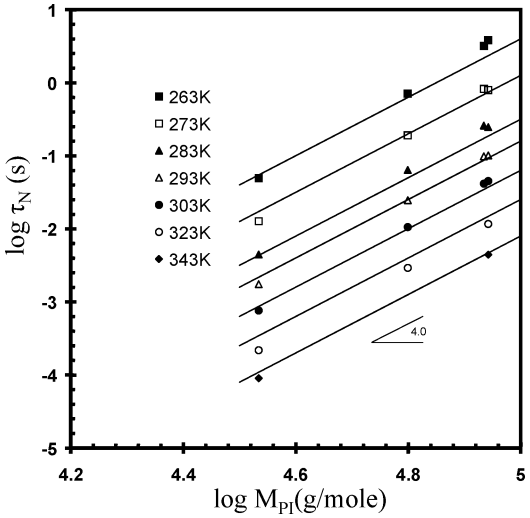

Figure 5. Dielectric normal mode relaxation time (τ_N) as a function of molecular weight (M_{PI}).

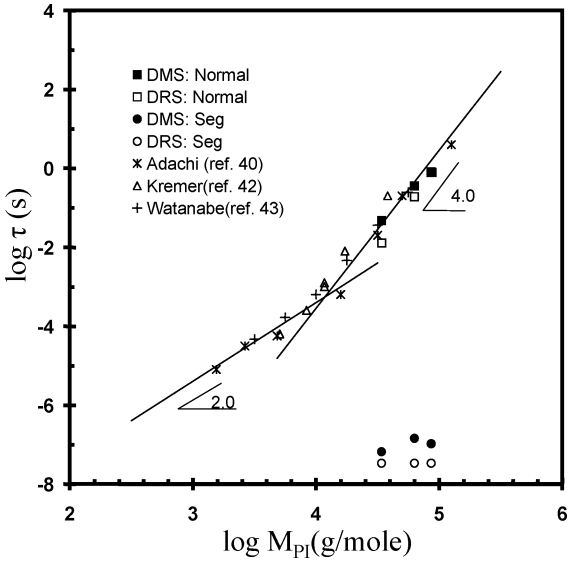

Figure 6. DMS and DRS relaxation times for segmental (τ_S) and normal (τ_N) mode as a function of molecular weight at 273 K. Code: filled circles and squares, τ_{SDMS} and τ_{NDMS} from this study; open circles and squares, τ_{SDRS} and τ_{NDRS} from this study; stars, data from ref 40; triangles, data from ref 42; plus (+), data from ref 43. Note the solid lines are fits for τ_N in the Rouse regime ($\tau_N \sim M^{2.0}$) and the reptation regime ($\tau_N \sim M^{4.0}$).

right of Figure 6, and the extrapolated value of τ_S from the VFT fits of the DRS results at 273 K is included for comparison. The DMS data are slightly scattered, and the DMS τ_S is longer than the extrapolated DRS τ_S. A similar finding was reported by Santangelo and Roland,[45] who pointed out that the difference in the frequency at maximum loss between DRS and DMS spectra is partly due to the fact that the retardation times are always longer than the corresponding relaxation times.

Multigraft Poly(isoprene-*graft*-styrene) Copolymers. Multigraft (MG) poly(isoprene-*graft*-styrene) copolymer is a nonlinear block copolymer with a varying number of PS grafts (1 for the *comb*, 2 for the *centipede*, and 4 for the *barbwire*) emanating from each branch point along the PI backbone. We stress that our MG copolymers differ from star polymers, where, as a rule, the same type of chain emanates from the central point. Thus, even the simplest *comb* (with one branch point) studied in this work differs from a three-arm star because different blocks (two PIs and one PS) are anchored at the branch point. In the schematics of Figure 1, where the three molecular architectures of MG copolymers investigated in this study are shown, the number of branch points for combs, centipedes, and barbwires was arbitrarily fixed at three. In the course of this work, however, we have prepared and tested a wide variety of MG copolymers with the number of branch points ranging from 2 to over 6 (see Table 1). Because of the dissimilarity of the two blocks in the MG copolymer, the samples are not in a homogeneous disordered state but rather in the form of microdomains. The glass transition temperature of the PI block, $T_{g,PI}$, is readily captured by DSC; the midpoint of the DSC trace for the PI transition is observed at 217 K for all MG copolymers. However, the T_g of the PS block, $T_{g,PS}$, is not as sharp; the transition occurs over a wide temperature range, and the $T_{g,PS}$ could be estimated from the Allen−Fox equation using the molecular weight of the PS block, M_{PS}:[56]

$$1/T_{g,PS} = 1/373 + 0.72/M_{PS} \quad \text{in K}^{-1} \qquad (2)$$

The thus calculated $T_{g,PS}$ are 372, 370, 367, and 365 K for *comb1*, *comb2*, *centipede*, and *barbwire*, respectively. The observed variation in the measured $T_{g,PS}$ of ±3 K must be considered quite small. The near constancy of $T_{g,PI}$ and $T_{g,PS}$ in samples of different molecular architecture suggests that the PI and PS microdomains are well separated in all MG copolymers.

We now focus attention on the principal theme of this study, i.e., the dynamics of the three families of MG copolymers with different molecular architecture: combs, centipedes, and barbwires. The presentation and discussion of our results are organized in the sequence designed to (1) establish the principal features of the dynamics of all MG copolymers, (2) compare the dynamics of each MG copolymer with those of its PI precursor, (3) examine the dynamics of MG copolymers with the same architecture (i.e., the same functionality of a branch point) but different molecular weights of PI and/or PS blocks, and (4) contrast the dynamics of MG copolymers of different architecture (i.e., different branch point functionality).

Principal Features of the Dynamics of MG Copolymers. The principal feature of the dielectric spectra of our MG copolymers is the presence of two readily distinguishable relaxation processes. This is exemplified in Figure 7, which illustrates dielectric loss in the frequency domain with temperature as a parameter for *comb2*. The normal mode (α_N, Figure 7A) and the segmental mode (α, Figure 7B) are shown separately for clarity. The local β process in PI is observed at the high-frequency end of Figure 7B. The relaxation strength of the normal mode decreases with temperature similar to that of the PI precursor (Figure 2B) though this is less obvious on the log scale of Figure 7A. The two processes are not always easily detectable in a single frequency sweep at a constant temperature; that depends on the molecular weight and architecture and will be discussed later in the text. Both processes reflect the relaxation motions of the PI blocks. The PS blocks affect the relaxation in the PI blocks but do not provide their own contribution to the measured dielectric response. (Frequency sweeps and temperature scans of the neat PS are uneventful.) The key point here is that spectra

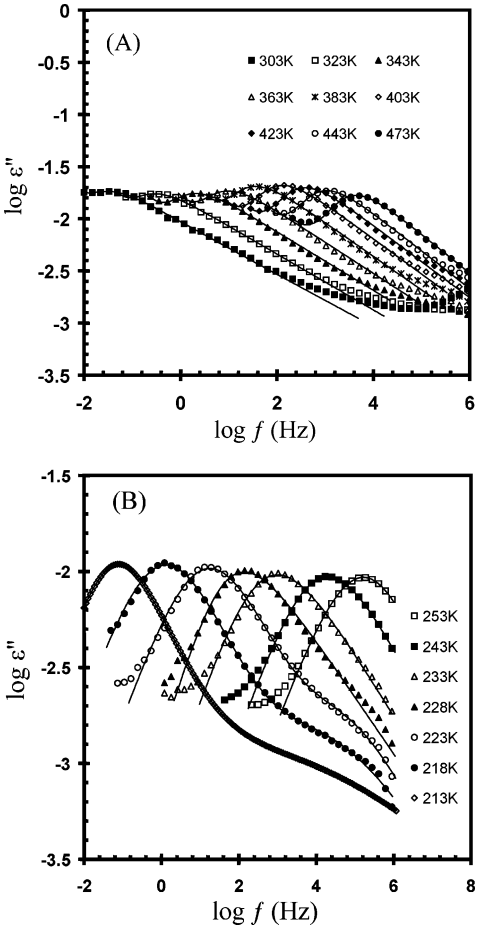

Figure 7. Dielectric loss for *comb2* in the frequency domain with temperature as a parameter: (A) normal mode; (B) segmental mode.

in Figure 7 typify the dielectric response of all MG copolymers investigated in this study—all are characterized by the presence of both segmental and normal mode processes that originate in the PI blocks.

Comparison of the Dynamics of MG Copolymer and Its PI Precursor. The next question we ask is how the segmental and normal mode processes in a MG copolymer compare with those in its PI precursor. This is best visualized and understood by contrasting the DRS spectra of a MG copolymer and its PI precursor. By way of example we select a representative pair of a MG copolymer (*barbwire*) and its PI precursor (PI2) but stress that analogous results were obtained for other MG copolymers and their PI precursors. Thus, the following example represents a general trend. Figure 8 shows dielectric loss in the frequency domain for the *barbwire* and PI2 measured at 243 K (open and filled squares) and 343 K (open and filled circles). The two measuring temperatures are chosen for convenience, and only four spectra are included in Figure 8 for clarity. The peaks appearing at higher frequency are obtained at lower temperature (243 K); they represent the segmental process in the PI precursor (filled squares) and the *barbwire* (open squares). We observe lower loss intensity in the *barbwire* but no change in the relaxation time for the segmental process between these two samples. The decrease in the intensity of the segmental loss peak can be attributed to the decrease in the concentration of PI segments in the *barbwire* compared to the neat PI. The observation that the segmental process in those two samples is characterized by the

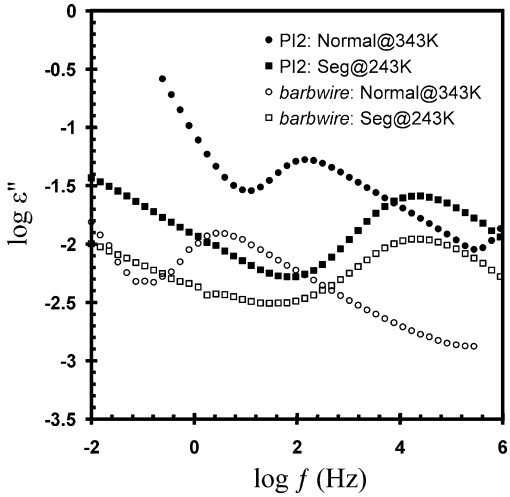

Figure 8. Dielectric loss for PI2 (filled symbols) and the *barbwire* (open symbols) in the frequency domain measured at 243 K (filled and open squares, segmental mode) and 343 K (filled and open circles, normal mode).

same relaxation time is not surprising. The contribution to the segmental process in the *barbwire* comes from the PI block. The time scale and the length scale of segmental motions in the PI blocks in the *barbwire* do not vary from those in the PI precursor. Since this finding was universal to all samples studied, it is safe to conclude that the relaxation time for the segmental process in all MG copolymers and PI precursors calculated from the HN fits (eq 1) falls on the same VFT curve and can be described by the parameters listed in Table 2. The segmental process is thermodielectrically simple in all MG copolymers over a wide range of temperature (and frequency).

As further seen in Figure 8, the normal mode process measured at 343 K gives rise to the dielectric dispersion at low frequency. Note that the relaxation time for the normal mode process in the *barbwire* (open circles) is longer than in the PI precursor (filled circles), and the loss peak intensity is decreased. The observed slowing down of the normal mode in the MG copolymer suggests that the relaxation of the PI blocks is affected by some form of confinement imposed by the PS microdomains. A comparison of the shape of the normal mode spectrum of a MG copolymer and its PI precursor yielded interesting results. Common to all normalized dielectric spectra was a perfect overlap on the low-frequency end. The high-frequency end was characterized by a slight broadening, though we were not able to establish a systematic trend as a function of molecular weight or molecular architecture. We hasten to add, however, that a different picture has emerged from the studies of linear diblock and triblock (BC) copolymers. For example, Yao et al.[22] reported that the distribution of the normal mode in styrene–isoprene diblock copolymers changed with molecular weight in the range from 4600 to 42 000 g/mol. They offered an explanation by considering two types of confinement, spatial and thermodynamic, for both nonentangled and entangled chains. Dielectric relaxation due to the global motion is also significantly retarded in the star vs linear PIs.[48] But the different trend observed in MG copolymers vis-à-vis BC copolymers and stars is not surprising considering the fundamental topological difference between these types of copolymers. The former have the same backbone and the latter do not, and that must affect the dynamics.

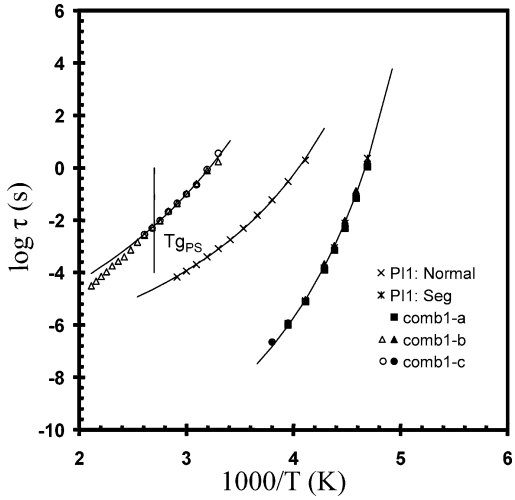

Figure 9. Temperature dependence of the relaxation time for normal and segmental mode in PI1 (stars and crosses symbols depict segmental and normal mode, respectively) and *comb1* (filled and open symbols depict segmental and normal mode, respectively).

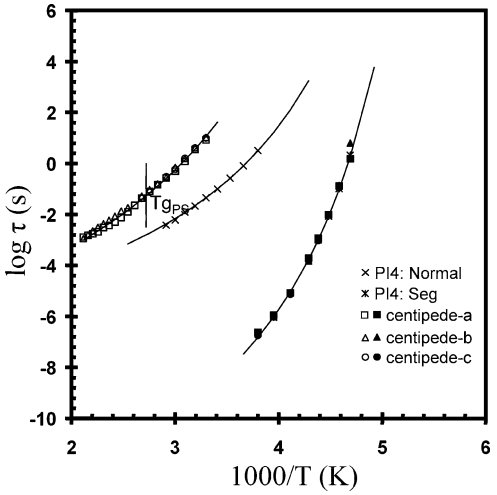

Figure 11. Temperature dependence of the relaxation time for normal and segmental mode in PI4 (stars and crosses depict segmental and normal mode, respectively) and the *centipede* (filled and open symbols depict segmental and normal mode, respectively).

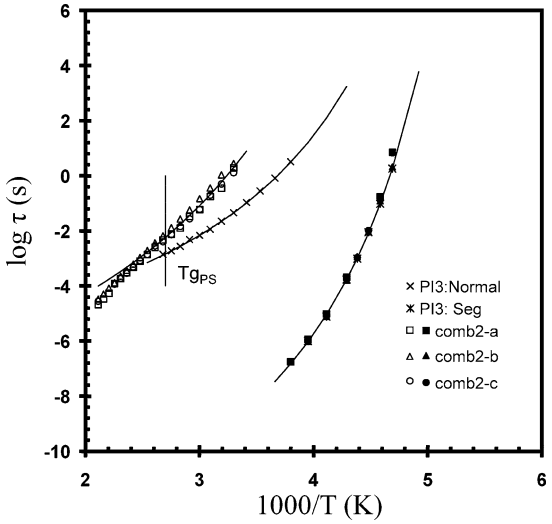

Figure 10. Temperature dependence of the relaxation time for normal and segmental mode in PI3 (stars and crosses depict segmental and normal mode, respectively) and *comb2* (filled and open symbols depict segmental and normal mode, respectively).

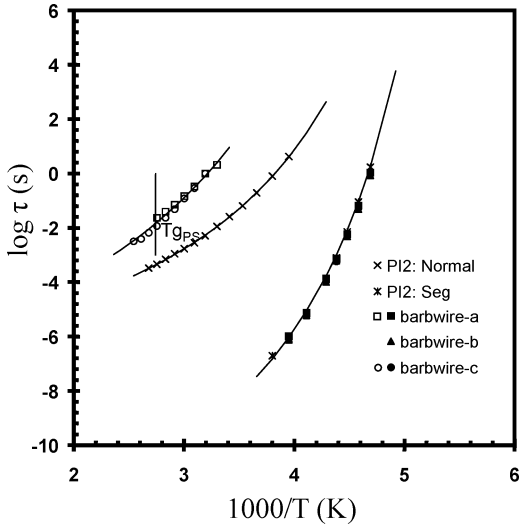

Figure 12. Temperature dependence of the relaxation time for normal and segmental mode in PI2 (stars and crosses depict segmental and normal mode, respectively) and the *barbwire* (filled and open symbols depict segmental and normal mode, respectively).

Dynamics of MG Copolymers with the Same Architecture But Different Molecular Weight (Same Functionality But Different Number of Branch Points). In this section we describe how an increase in the overall molecular weight (or an increase in the *number* of branch points) affects the dynamics of each of the three architectures investigated: *combs*, *centipedes*, and *barbwires*. We start by examining the temperature dependence of the relaxation time for each molecular architecture. A large number of frequency sweeps were conducted on all MG copolymers over a broad range of frequency and temperature. The data were collected, analyzed, and plotted in Figures 9−12 which show the temperature dependence of the relaxation time for normal and segmental mode for *comb1* (Figure 9), *comb2* (Figure 10), *centipede* (Figure 11), and *barbwire* (Figure 12). Also included in each figure are the data for the corresponding PI precursor. The solid lines in Figures 9−12 are best fits to the VFT equation; the corresponding VFT parameters for the PI precursors and MG copolymers are given in Table 2. For completion, Table 2 also contains the molecular weights of the PI and PS blocks and the number of PS grafts per branch point. Note that the Vogel temperature remains unchanged while τ_{N0} varies within 1 order of magnitude. The constant related to the activation energy of the relaxation process, B ($B = E_a/K_B$), varies for MG copolymers but remains constant for the PI precursors. The data for the segmental process, which is independent of molecular weight and molecular architecture, are included in Figures 9−12 for completion and also in order to facilitate the distinction between the time scales of segmental and normal modes.

We have already established (Figure 9) that the normal mode process in a MG copolymer differs from that in the corresponding neat PI precursor; we shall now address this result in more detail. The two principal findings regarding the normal mode are (1) the relaxation time for the normal mode process is longer in the MG copolymers than in the corresponding PI precursor

and (2) the relaxation time for the normal mode process in MG copolymer of a given architecture is not a function of the overall molecular weight, M.

We estimate that the measured increase in τ_N in copolymers could be realized in the neat PI by increasing the molecular weight by a factor of 2−3. It is interesting to note that, notwithstanding the difference in the molecular architecture, this finding is analogous to the results reported by Yao et al. for linear styrene−isoprene (SI) BCs,[22] Floudas et al. for star copolymers,[33] and Watanabe et al. for monodisperse linear PI stars.[48] Floudas et al.[33] also studied four-arm star BCs, with each arm composed of PI and PS blocks. For the resulting systems, self-assembled in the form of the PI core and the PS corona, they found that the difference between τ_N in the star polymer and the PI precursor depended on M_{PI}. For $M < M_e$, there was little difference in the relaxation rate, but for $M \sim 3M_e$, τ_N in the star polymer was about 1−2 orders *faster* than in the PI precursor. The faster dynamics are due to the fluctuations of a part of the chain including the star center within a restricted space.

With regard to the first finding, an intriguing question is, what slows down the normal mode in MG copolymers? There is little doubt that some form of confinement exerted by the PS blocks plays a role, though the exact mechanism is not clear. Intuitively, we expected that glassy and rubbery PS domains would affect the PI dynamics differently, and hence our first goal was to probe the normal mode dynamics above and below the glass transition of PS ($T_{g,PS}$). The DSC $T_{g,PS}$ is marked by the vertical bar in Figures 9−12. We have observed some intriguing results, particularly above the $T_{g,PS}$. For example, we find that the experimental data above the $T_{g,PS}$ fall off the VFT fits for some MG copolymers; this trend is particularly pronounced in *comb1* (Figure 9) and *comb2* (Figure 10). In the *barbwire*, however, we could not get sufficiently reliable data at higher temperature due to high conductivity, while the data for the *centipede* at higher temperature could be fit to either a straight line or a VFT form. The observed trend is curious, and the simplest rationalization can be offered by invoking the temperature dependence of the mobility of the PS blocks in MG copolymers. Below the $T_{g,PS}$, the PI chain ends are tethered to the glassy PS microdomains: two ends are tethered for the intermediate PI spacer, and one end is tethered for the PI blocks at each end of the chain. The PI blocks tethered at one end contribute to the normal mode relaxation. The PI segments tethered at both ends are also believed to contribute to the chain fluctuations, although that is difficult to quantify. The likelihood that this will materialize increases with the increase in the weight fraction of the PI blocks, and an analogy to a spring and bead mechanism could be invoked. This is further corroborated by our results on epoxy-terminated PPO/amine networks where we observe the normal mode process in the PPO well below the T_g of the DGEBA spacer, even though the PPO chains are tethered to DGEBA at both ends.[58] Nonetheless, the ensuing relaxation of the PI block is impeded by the glassy PS microdomains resulting in the observed slowdown in the relaxation of MG copolymers vis-à-vis the PI precursors. As the $T_{g,PS}$ is approached, the experimentally measured gap between the relaxation time for MG copolymer and PI precursor decreases because of the increased mobility of the PS microdomains and, by extension, the branch points. Above the $T_{g,PS}$, the mobility of the tethered points increases still further. That gives rise to an effective increase in the relaxation rate and a decrease in the relaxation time, resulting in the observed convergence of the relaxation times for the MG copolymer and the PI precursor, particularly evident in Figures 9 and 10. It is very curious, however, that the relaxation time at high-temperature crosses over the extrapolated VFT fit of its PI precursor (Figures 9 and 10). This is an interesting subject for further study.

The observed increase in the relaxation time for a MG copolymer could not be attributed to an increase in the molecular weight of the PI block because the same spacer (same M_{PI}) is used in a MG copolymer and its precursor. What are then the possible mechanisms that would effectively increase τ_N in MG copolymers vis-à-vis the PI precursors? One possible explanation could be formulated as the consequence of the reduced mobility of PS microdomains. This is particularly true at lower temperature, below the $T_{g,PS}$, where the thermally quenched PS microdomains contract (densify) and the tethered PI chains are effectively stretched out. That, in turn, would translate into an increase in the end-to-end displacement vector and the relaxation time because τ_N is proportional to $\langle r^2\rangle^{1/2}$ via the cumulative vector component of the dipole moment along the chain contour. The implication is that the PI spacer in a MG copolymer experiences its own distinct "effective" $\langle r^2\rangle^{1/2}$, different from that in the PI precursor. This effect diminishes with increasing temperature because the mobility of the PS microdomains increases, as evidenced by the observed convergence of the relaxation times for the MG copolymer and the PI precursor. This also brings to mind an analogy with strongly segregated block copolymers, where stretching is the consequence of the balancing tendency to decrease interfacial tension with decreasing configurational entropy. An alternative mechanism for the increase in τ_N could be attributed to an increase in the dielectric cross-correlations contained in the Kirkwood correlation function[57] between the PI chains in a MG copolymer. A similar finding has been recently reported in polymer networks where one reactive component was a type A chain.[58]

The second major finding in Figures 9−12 is that the relaxation time for the normal mode in a MG copolymer of a given architecture is not a function of the overall molecular weight or the number of branch points. The implication is clear; the normal mode process in combs, centipedes, and barbwires scales with the "effective" molecular weight of the PI spacer and not the overall molecular weight of the MG copolymer.

The results of dynamic mechanical spectroscopy (DMS) for each architecture of MG copolymers are examined next. Master curves for storage (G') and loss modulus (G'') in the frequency domain at a reference temperature of 218 K for *comb2-a* and *comb2-c* are shown in parts A and B of Figure 13. The data for the *centipede* and the *barbwire* do not coalesce on a master curve and are not shown here. The plateau modulus (G_N) for *comb2-a* and *comb2-c* was determined from Figure 13A by taking the value of the onset of transition from segmental to terminal mode. The thus obtained value is 5.01×10^5 Pa is slightly higher than that of the neat PI precursors (3.5×10^5 Pa). The reported data[59] list the plateau modulus in PS at 2.0×10^5 Pa and the M_e of PS at 13 300 g/mol. The higher value of plateau modulus in

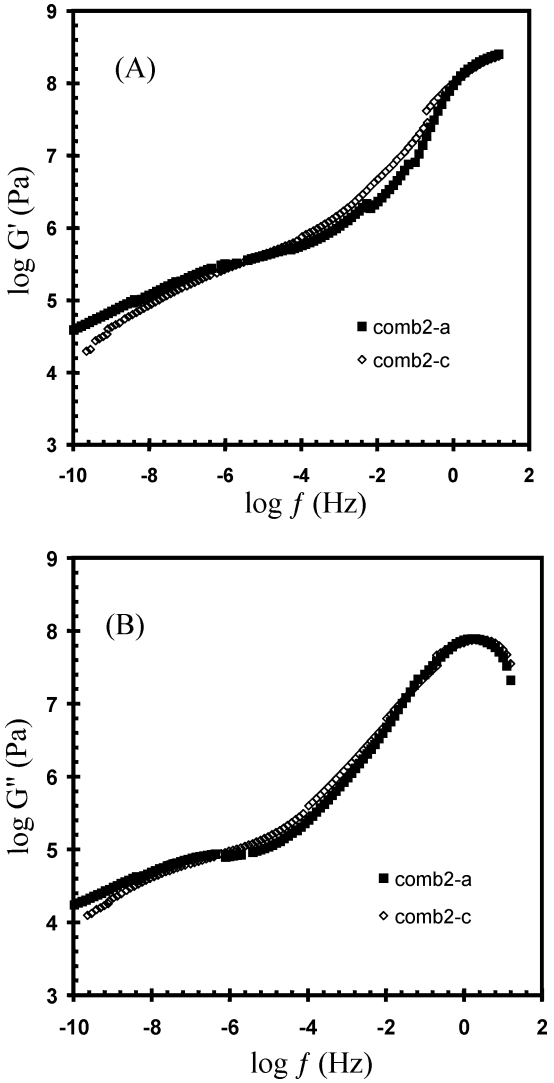

Figure 13. Storage modulus (A) and loss modulus (B) in the frequency domain for *comb2-a* and *comb2-c* at a reference temperature of 218 K.

combs than in the PI and PS precursors suggests that the M_e of combs is lower and the monomeric friction coefficient higher than the corresponding values in the precursors. The zero-shear viscosity (η_0) was extracted directly from the data by averaging the low shear rate values of η. The average value of the terminal relaxation time, τ_1, was calculated from the DMS data using the following relationship:

$$\tau_1 \equiv \frac{\eta_0}{G_N} = \frac{\sum_p \tau_{G,p} h_p}{\sum_p h_p} \qquad (3)$$

The chain dynamics (expressed in terms of τ_N from DRS and τ_1 from DMS) of *comb2* as a function of reciprocal temperature are illustrated in Figure 14. The segmental relaxation data are included for completion. The two fractions of the comb architecture, *comb2-a* and *comb2-c*, have different terminal relaxation times. The longer relaxation time is found in a higher molecular weight sample, *comb2-a*. This difference is pronounced at lower temperature, and it diminishes with increasing temperature. That DMS data for τ_N appear below the

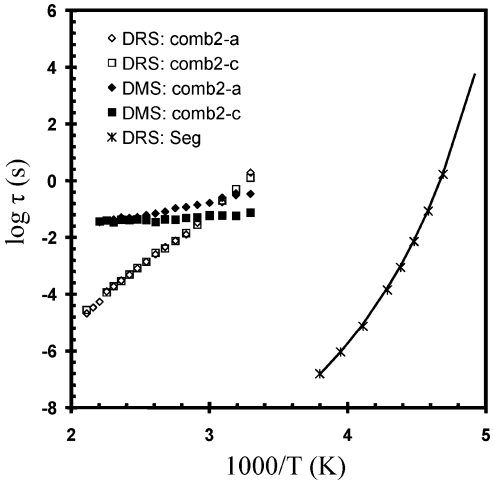

Figure 14. Temperature dependence of the relaxation time for normal mode in *comb2-a* and *comb2-c* obtained from DRS (open symbols) and DMS (filled symbols) measurements. DRS segmental mode (stars) is shown for comparison.

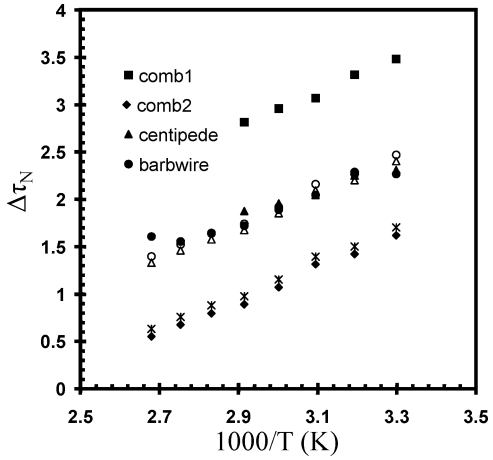

Figure 15. $\Delta\tau_N$ (defined as $\tau_{N(PIPS)} - \tau_{N(PI)}$) for *comb1*, *comb2*, *centipede*, and *barbwire* as a function of reciprocal temperature. Note: filled symbols are obtained from measured data; open circles are interpolated data for comb with $M_{PS} = 52\,000$ g/mol; stars and open triangles are interpolated data for comb with $M_{PS} = 33\,600$ and 50 400 g/mol, respectively. For detailed explanation see the text.

DMS data for τ_1 is not surprising considering that the length scale of the DRS measure is associated with the PI block, while the length scale of the DMS measure corresponds to the entire MG molecule. It is therefore logical that τ_1 is longer than τ_N. A curious observation is that, at temperatures well below the $T_{g,PS}$, τ_1 crosses over the τ_N line.

Dynamics of MG Copolymers of Different Architecture (Different Functionality of Branch Points). We have shown above that the overall molecular weight (and hence the number of branch points) does not affect the dynamics of MG copolymers of a given architecture. We now proceed to investigate the effect of other molecular parameters on the copolymer dynamics, such as the length of a PS graft (M_{PS}) and the number of PS grafts per branch point. We define $\Delta\tau_N$ as the difference between the normal mode relaxation time for each MG copolymer, $\tau_{N(PIPS)}$, and its PI precursor, $\tau_{N(PI)}$. We calculate $\Delta\tau_N$ from $\Delta\tau_N = \tau_{N(PIPS)} - \tau_{N(PI)}$ and plot it as a function of reciprocal temperature in Figure 15. The following principal observations are made within the experimental range of temperature

and frequency used in this study: (1) $\Delta\tau_N$ is always positive, i.e., $\tau_{N(PIPS)} > \tau_{N(PI)}$; (2) $\Delta\tau_N$ increases with decreasing temperature; (3) the rate of change of $\Delta\tau_N$ with temperature is the same for all MG copolymers; and (4) the magnitude of $\Delta\tau_N$ varies as a function of molecular architecture. Careful examination of Figure 15 affords a closer look at the effect of molecular architecture on $\Delta\tau_N$. Note that the original data for the four MG copolymers in Figure 15 are represented by filled symbols. As stated above, we were particularly interested in establishing which specific aspect of molecular architecture plays the key role in dynamics. The effect of the length (M_{PS}) of a PS graft is examined first by comparing samples with the same architecture but different M_{PS}. This requirement is met for the two combs: *comb1* (M_{PS} = 31 600 g/mol) and *comb2* (M_{PS} = 77 300 g/mol; see Table 1). The subtraction of $\tau_{N(PI)}$ from $\tau_{N(PIPS)}$ takes into account the difference in the M_{PI} between *comb1* and *comb2*. It is immediately clear from Figure 15 that the length of the PS graft (M_{PS}) has a strong effect on $\Delta\tau_N$: a considerable increase in $\Delta\tau_N$ is recorded with an increase in M_{PS} from 31 600 to 77 300 g/mol. The data for *comb1* and *comb2* in Figure 15 represent the upper and the lower limit of $\Delta\tau_N$, respectively. The data for the *centipede* and the *barbwire* fall in the middle of Figure 15, and we tried to rationalize those findings in terms of their M_{PS}. The *barbwire* has four PS grafts, each with M_{PS} = 13 000 g/mol; hence, the total molecular weight of PS emanating from one branch point is 13 000 × 4 = 52 000 g/mol. If we consider a comb with one PS graft with M_{PS} = 52 000 g/mol and calculate $\Delta\tau_N$ by simple intrapolation between the measured limits for *comb1* (31 600 g/mol) and *comb2* (77 300 g/mol), the resulting value coincides with that for the *barbwire*. This is an impressive finding in support of the hypothesis that the key factor that determines the magnitude of $\Delta\tau_N$ is the total molecular weight of all PS grafts emanating from a single branch point. Of course, the assumption of linear intrapolation is an approximation because $\Delta\tau_N$ is bound to reach an asymptotic limit with increasing molecular weight. But a similar calculation for the *centipede*, with M_{PS} = 16 800 g/mol and the total molecular weight of PS per branch point of 16 800 × 2 = 33 600 g/mol, underestimates the measured value. The observed discrepancy, however, could be accounted for by the topological irregularities in the *centipede* resulting from the synthesis. The reported[37] formation of IS_3 branch points results in an effective increase in the average number of PS grafts per branch point that could explain the experimental results. In sum, the hitherto obtained results point out the key role of the total molecular weight of the graft block per branch point in the MG copolymer dynamics. By way of example, assuming that the total molecular weight of the PS graft block per branch unit governs the dynamics, we would expect the following three samples of different molecular architecture to have the same $\Delta\tau_N$: a *comb* with a single PS graft with M_{PS} = 40 000 g/mol, a *centipede* with two PS grafts, each with M_{PS} = 20 000 g/mol, and a *barbwire* with four PS grafts, each with M_{PS} = 10 000 g/mol. A further study along those lines would be of interest.

Morphological Considerations. A detailed study of the morphology of our MG copolymers was beyond the scope of this article, and we shall limit ourselves to some initial consideration that, nonetheless, proved interesting. While the morphology of linear block copolymers (with immiscible blocks) is characterized by prominent microphase separation and is well understood,[60−62] the same cannot be said for the MG copolymers. Apparently, the morphology of nonlinear MG blocks is a more complex function of the molecular architecture and the volume fraction of block components. On the basis of theoretical considerations, Milner[63] has constructed a phase diagram for simple $A_{n_A}B_{n_B}$ star block copolymers, where n_A and n_B represent the number of arms of blocks A and B. His diagram affords prediction of the microphase morphology (spherical, cylindrical, bicontinuous, or lamellar) in those copolymers based upon the knowledge of a chain architecture parameter, termed ϵ, and a volume fraction of one block, ϕ. The parameter ϵ is defined as $\epsilon = (n_A/n_B)(l_A/l_B)^{1/2}$, where l_A and l_B are material parameters defined as $l_i = V_i/R_i^2$, and V_i and R_i are the molecular volume and the radius of gyration of the respective blocks (i = A or B). Several groups[64−68] reported attempts to extend Milner's phase diagram to more complex molecular architectures, including MG copolymers of PI and PS. Gido et al.[66] compared the experimental results obtained by transmission electron microscopy (TEM) with the prediction of Milner's phase diagram. They considered the so-called H-shaped and π-shaped architecture; the former corresponds to a portion of our centipede consisting of one PI spacer and two PS grafts at each end, while the latter corresponds to our comb with two functional branch points. They start by assuming that each MG copolymer is composed of simple building block grafts that conform to Milner's phase diagram and proceed to modify Milner's theory by incorporating a new parameter τ, defined as the fractional distance along the A backbone at which the B graft occurs. They postulated the relationship $\epsilon = f(\tau)(l_A/l_B)^{1/2}$ for a MG copolymer and determined the morphological boundaries within which their H-shaped and π-shaped copolymers were located on the phase diagram. Our MG copolymers are characterized by an even more complex architecture; nonetheless, following Milner[68] and Gido et al.,[66] we have performed a similar analysis, and a brief recap of our salient findings is as follows. For our MG copolymers, the *combs*, the *centipede*, and the *barbwire*, we define a building block by a virtual cut of the PI backbone halfway between the branch points. That enables us to consider our samples as being composed of sets of simple starlike constituents: ISI for the *combs*, IS_2I for the *centipede*, and IS_4I for the *barbwire*. Here "I" represents the PI segment, "S" represents the PS segment, and the numerical subscript depicts the number of PS segments emanating from a branch point. For MG copolymers with two branch points a cut in the middle of the PI backbone between the branch points produces two asymmetric constituents with $\tau \cong 0.35$. For MG copolymers with the number of branch points in excess of two, we first cut off one-half of the PI spacer at each end and then follow by subsequent cuts in the middle between the branch points. That yields constituents with symmetric structure and $\tau = 0.5$. On the basis of the segmental volumes (132 and 176 Å^3 for PI and PS, respectively[69]) and the statistical chain lengths (6.8 and 6.9 Å for PI and PS, respectively[70]), we calculated the value of $(l_{PI}/l_{PS})^{1/2}$ equal to 0.89. The relationship $\epsilon = f(\tau)(l_A/l_B)^{1/2}$ represents linear block copolymers [$\epsilon = (l_A/l_B)^{1/2}$] for τ = 0 or 1 and a simple symmetric graft [$\epsilon = 2(l_A/l_B)^{1/2}$] for $\tau = 0.5$. In between those limits the value of ϵ is not a priori known but should be a continuous function. Following Gido et

Table 3. Predicted Morphology of MG Copolymers Based on Milner's Phase Diagram

materials	ϕ_{PS}	no. of branch points	τ	$\epsilon = f(\tau)(l_A/l_B)^{1/2}$	morphology
comb1-a	65.4	3.7	0.5	1.78	lamella
comb1-b	67.2	2.6	0.5	1.78	lamella
comb1-c	67.8	2.0	0.35	1.39−1.78	lamella
comb2-a	18.4	3.5	0.5	1.78	sphere
comb2-b	19.0	2.7	0.5	1.78	sphere
comb2-c	19.0	2.1	0.35	1.39−1.78	sphere
centipede-a	24.9	6.6	0.5	1.12	cylinder
centipede-b	24.7	4.4	0.5	1.12	cylinder
centipede-c	24.5	2.2	0.5	1.12	cylinder
barbwire-a	38.3	3.0	0.5	2.25	lamella
barbwire-b	37.9	2.3	0.5	2.25	lamella
barbwire-c	38.2	1.9	0.5	2.25	lamella

al.[66] and using the allowable range of $f(\tau)$ values, the calculated value of ϵ and the known volume fraction of one block, ϕ_i, we were able to suggest the possible morphologies of our MG copolymers using the predictions of Milner's theory. We note that in the calculations for combs we use $(l_{PI}/l_{PS})^{1/2}$ while for centipedes and barbwires we use $(l_{PI}/l_{PS})^{-1/2}$in order to ensure that $\epsilon > 1$. The predicted morphologies for our MG copolymers—combs, centipedes, and barbwires—are listed in Table 3. In Gido's study,[66] π architecture copolymer with 0.21 volume fraction of PS yields morphology composed of spherical PS microdomains in a PI matrix. We arrive at the same conclusion for our combs (reduced to π architecture when branch points are 2) with 0.19 volume fraction of PS and the number of branch points from 2 to 3.7. For the larger PS volume fraction of 0.67, we predict that the combs should have lamellar morphology. Beyer et al.[68] also studied the centipede architecture with 4.4−9.2 branch points and the volume fraction of PS of 0.21. The predicted cylindrical morphology was observed by TEM, and the domain shape was conserved, although the long-range order was found to decrease with increasing molecular weight or the number of branch points. A TEM study of our samples would be desirable in the future to further aid the interpretations of the dynamics observed here.

In the context of the present study, however, the key question is whether the morphology affects the dynamics at all. The segmental process, with its short time scale and length scale, is not affected by morphology, and that is borne out by our results for a gamut of MG copolymers of varying molecular weight, volume fraction of the blocks, and molecular architecture. The (longer scale) dielectric normal mode process should be, in principle, more sensitive to its morphological milieu. But the precise nature of the effect of the interplay between the molecular architecture and the morphology of self-assembled microdomains on the dielectric normal mode dynamics is complex and remains incompletely understood. Some insight is obtained from this work; however, a complete answer to that query requires a study on a wider series of MG copolymers with systematically varying block volume fraction and molecular architecture. Finally, the terminal dynamics evaluated from rheological measurements depend on morphology; studies along those lines have been reported for linear BCs[71] but not for MG copolymers. These are interesting subjects for future research.

Conclusions

In this article we have described the effect of molecular weight and molecular architecture of three types of multigraft (MG) copolymers, namely *combs*, *centipedes*, and *barbwires*, on their dynamics. Regularly spaced MG copolymers were prepared from PI and PS precursors by anionic polymerization.

PI precursor is a typical type A polymer, characterized by both segmental and normal mode relaxations. Both processes are thermodielectrically simple, and the temperature dependence of their relaxation times is of the Vogel−Fulcher−Tammann (VFT) type. The dielectric normal mode relaxation time, τ_N, was found to obey the relationship τ_N proportional to $M^{4.0}$.

MG copolymers were characterized by well-separated microdomains; the DSC T_g of each microdomain was practically identical to that of the corresponding neat component. The two relaxation processes observed in the PI precursors, namely segmental and normal mode, were also readily distinguishable in the dielectric spectra of all MG copolymers. The segmental process did not change as a function of molecular weight or molecular architecture, suggesting that the time scale and the length scale of segmental motions in the PI blocks in the copolymer do not differ from those in the precursor. But the normal mode process in MG copolymers slows down and shifts to lower frequency (i.e., τ_N increases) in comparison to that in the PI precursor. Two possible mechanisms that would cause an increase in τ_N were suggested. One explanation was offered on the basis of the reduced mobility of PS microdomains, which is particularly important below the $T_{g,PS}$. The thermally quenched PS microdomains contract (densify) and the tethered PI chains are effectively stretched out, resulting in an increase in the end-to-end displacement vector and the relaxation time, because τ_N is proportional to $\langle r^2\rangle^{1/2}$. The implication is that the PI spacer in a MG copolymer experiences its own distinct "effective" $\langle r^2\rangle^{1/2}$, different from that in the PI precursor: consequently, the normal mode process in *combs*, *centipedes*, and *barbwires* scales with the "effective" molecular weight of the PI spacer and not the overall molecular weight of the MG copolymer. This effect diminishes with increasing temperature because the mobility of the PS microdomains increases, as evidenced by the observed convergence of the relaxation times for the MG copolymer and the PI precursor. An alternative mechanism for the increase in τ_N could be attributed to an increase in the cross-correlations between the PI chains in a MG copolymer. A similar finding has been recently reported in polymer networks where one reactive component was a type A chain.[58]

The effect of molecular architecture on the dynamics was quantified in terms of $\Delta\tau_N$, the difference between the normal mode relaxation time for each MG copolymer, $\tau_{N(PIPS)}$, and its PI precursor, $\tau_{N(PI)}$. Thus, $\Delta\tau_N = \tau_{N(PIPS)} - \tau_{N(PI)}$. The following principal observations are made within the experimental range of temperature and frequency used in this study: (1) $\Delta\tau_N$ is always positive, i.e., $\tau_{N(PIPS)} > \tau_{N(PI)}$; (2) $\Delta\tau_N$ increases with decreasing temperature; (3) the rate of change of $\Delta\tau_N$ with temperature is the same for all MG copolymers; and (4) the magnitude of $\Delta\tau_N$ varies as a function of molecular architecture. The results generated in this work identify the total molecular weight of the PS grafts emanating from a single branch point as the principal factor that affects the MG copolymer dynamics.

Acknowledgment. This material is based on work supported by National Science Foundation under Grants

DMR-0101182 and DMR-9975592. Work at the University of Tennessee (J.W.M.) was supported by the U.S. Army Research Office (DAAGD19-01-1-0544). We thank Professor Dejan Zečević of The Yale University Medical School for revealing insight into analogies with biological systems.

References and Notes

(1) Most recent extensive accounts of dynamics in polymeric systems can be found in the following special issues: (a) *J. Phys.: Condens. Matter* **2003**, *15* (11); (b) *J. Non-Cryst. Solids* **2002**, 307−310. (c) Proceedings of the 2nd International Conference on Broadband Dielectric Spectroscopy and Its Applications, Leipzig, Germany, Sept 2−6, 2002. (d) *J. Phys. Chem.* **1999**, *103*.
(2) Adachi, K.; Kotaka, T. *Macromolecules* **1983**, *16*, 1936.
(3) Adachi, K.; Kotaka, T. *Macromolecules* **1985**, *18*, 295.
(4) Adachi, K.; Kotaka, T. *Macromolecules* **1987**, *20*, 2018.
(5) Adachi, K.; Kotaka, T. *Macromolecules* **1988**, *21*, 157.
(6) Ngai, K. L.; Rendell, R. W. *Polym. Prepr.* (*Am. Chem. Soc., Div. Polym. Chem.)* **1989**, *30*, 89.
(7) Boese, D.; Kremer, F.; Fetters, L. J. *Macromolecules* **1990**, *23*, 1826.
(8) Boese, D.; Kremer, F.; Fetters, L. J. *Polymer* **1990**, *31*, 1831.
(9) Patel, S. S.; Takahashi, K. M. *Macromolecules* **1992**, *25*, 4382.
(10) Watanabe, H.; Yamada, H.; Urakawa, O. *Macromolecules* **1995**, *28*, 6443.
(11) Roland, C. M.; Bero, C. A. *Macromolecules* **1996**, *29*, 7521.
(12) Adachi, K. In *Dielectric Spectroscopy of Polymeric Materials*; Runt, J. P., Fitzgerald, J. J., Eds.; American Chemical Society: Washington, DC, 1997; Chapter 9, pp 261−282.
(13) For excellent recent reviews see: (a) Watanabe, H. *Prog. Polym. Sci.* **1999**, *24*, 1253. (b) Watanabe, H. *Macromol. Rapid Commun.* **2001**, *22*, 127.
(14) Stockmayer, W. H.; Baur, M. E. *J. Am. Chem. Soc.* **1964**, *86*, 3485.
(15) Baur, M. E.; Stockmayer, W. H. *J. Chem. Phys.* **1965**, *43*, 4319.
(16) Stockmayer, W. H. *Pure Appl. Chem.* **1967**, *15*, 539.
(17) Kremer, F., Schonhals, A., Eds.; *Broadband Dielectric Spectroscopy*; Springer-Verlag: Berlin, 2002; p 261.
(18) Beevers, M. S.; Elliott, D. A.; Williams, G. *Polymer* **1979**, *20*, 785.
(19) Beevers, M. S.; Elliott, D. A.; Williams, G. *Polymer* **1980**, *21*, 13.
(20) Burke, J. J.; Stockmayer, W. H. *Macromolecules* **1969**, *2*, 647.
(21) Adachi, K.; Kotaka, T. *Prog. Polym. Sci.* **1993**, *18*, 585.
(22) Yao, M.-L.; Watanabe, H.; Adachi, K.; Kotaka, T. *Macromolecules* **1991**, *24*, 2955.
(23) Alig, I.; Kremer, F.; Fytas, G.; Roovers, J. *Macromolecules* **1992**, *25*, 5277.
(24) Stuhn, B.; Stickel, F. *Macromolecules* **1992**, *25*, 5306.
(25) Fytas, G.; Rizos, A.; Alig, I.; Kremer, F.; Roovers, J. *Polymer* **1993**, *34*, 2263.
(26) Johnson, J. M.; Allgaier, J. B.; Wright, S. J.; Young, R. N.; Buzza, M.; McLeish, T. C. B. *J. Chem. Soc., Faraday Trans.* **1995**, *91*, 2403.
(27) Patel, S. S.; Larson, R. G.; Winey, K. I.; Watanabe, H. *Macromolecules* **1995**, *28*, 4313.
(28) Sato, T.; Watanabe, H.; Osaki, K.; Yao, M.-L. *Macromolecules* **1996**, *29*, 3881.
(29) Alig, I.; Floudas, G.; Avgeropoulos, A.; Hadjichristidis, N. *Macromolecules* **1997**, *30*, 5004.
(30) Adachi, K.; Kotaka, T. *Pure Appl. Chem.* **1997**, *69*, 125.
(31) Zhang, Y.; Wiesner, U. *Macromol. Chem. Phys.* **1998**, *199*, 1771.
(32) Pispas, S.; Floudas, G.; Hadjichristidis, N. *Macromolecules* **1999**, *32*, 9074.
(33) Floudas, G.; Paraskeva, S.; Hadjichristidis, N.; Fytas, G.; Chu, B.; Semenov, A. N. *J. Chem. Phys.* **1997**, *107*, 5502.
(34) Poh, B. T.; Adachi, K.; Kotaka, T. *Macromolecules* **1996**, *29*, 6317.
(35) Sakurai, S.; Umeda, H.; Yoshida, A.; Nomura, S. *Macromolecules* **1997**, *30*, 7614.
(36) Floudas, G.; Meramveliotaki, K.; Hadjichristidis, N. *Macromolecules* **1999**, *32*, 7496.
(37) Uhrig, D.; Mays, J. W. *Macromolecules* **2002**, *35*, 7182.
(38) Fitz, B.; Andjelic, S.; Mijović, J. *Macromolecules* **1997**, *30*, 5227.
(39) Mijović, J.; Miura, N.; Monetta, T.; Duan, Y. *Polym. News* **2001**, *26*, 251.
(40) Imanishi, Y.; Adachi, K.; Kotaka, T. *J. Chem. Phys.* **1988**, *89*, 7585.
(41) Hirotsugu, Y.; Adachi, K.; Watanabe, H.; Kotaka, T. *Polym. J.* **1989**, *21*, 863.
(42) Boese, D.; Kremer, F. *Macromolecules* **1990**, *23*, 829.
(43) Yoshida, H.; Watanabe, H.; Adachi, K.; Kotaka, T. *Macromolecules* **1991**, *24*, 2981.
(44) Adachi, K.; Hirano, H. *Macromolecules* **1998**, *31*, 3958.
(45) Santangelo, P. G.; Roland, C. M. *Macromolecules* **1998**, *31*, 3715.
(46) Floudas, G.; Gravalides, C.; Reisinger, T.; Wegner, G. *J. Chem. Phys.* **1999**, *111*, 9847.
(47) Matsumiya, Y.; Watanabe, H.; Osaki, K. *Macromolecules* **2000**, *33*, 499.
(48) Watanabe, H.; Matsumiya, Y.; Osaki, K. *J. Polym. Sci., Part B: Polym. Phys.* **2000**, *38*, 1024.
(49) Matsumiya, Y.; Watanabe, H. *Macromolecules* **2001**, *34*, 5702.
(50) Watanabe, H.; Matsumiya, Y.; Inoue, T. *Macromolecules* **2002**, *35*, 2339.
(51) The fundamental aspects of DRS, theoretical and experimental, are well established, and the interested reader is referred to an excellent recent book: Kremer, F., Schonhals, A., Eds.; *Broadband Dielectric Spectroscopy*; Springer-Verlag: Berlin, 2002, and several excellent reviews: (a) Williams, G. Dielectric relaxation spectroscopy of amorphous polymer systems: the modern approaches. In *Keynote Lectures in Selected Topics of Polymer Science*; Riande, E., Ed.; CSIC: Madrid, 1997; Chapter 1, pp 1−40. (b) Williams, G. Theory of dielectric properties. In *Dielectric Spectroscopy of Polymeric Materials*; Runt, J. P., Fitzgerald, J. J., Eds.; American Chemical Society: Washington, DC, 1997; Chapter 1, pp 3−65.
(52) Havriliak, S., Jr.; Negami, S. *Polymer* **1967**, *8*, 161.
(53) Davidson, D. W.; Cole, R. H. *J. Chem. Phys.* **1950**, *18*, 1417.
(54) Williams, G.; Watts, D. C. *Trans. Faraday Soc.* **1970**, *66*, 80.
(55) Gotro, J. T.; Graessley, W. W. *Macromolecules* **1984**, *17*, 2767.
(56) Allen, V. R.; Fox, T. G. *J. Chem. Phys.* **1964**, *41*, 337.
(57) McCrum, N. G.; Read, B. E.; Williams, G. *Anelastic and Dielectric Effects in Polymeric Solids*; Dover Publications Inc.: New York, 1991.
(58) Mijović, J.; Han, Y.; Sun, M.; Pejanović, S. *Macromolecules* **2003**, *36*, 4589.
(59) Fetters, L. J.; Lohse, D. J.; Richter, D.; Witten, T. A.; Zirkel, A. *Macromolecules* **1994**, *27*, 4639.
(60) Bates, F. S.; Fredrickson, G. H. *Annu. Rev. Phys. Chem.* **1990**, *41*, 525.
(61) Fredrickson, G. H.; Bates, F. S. *Annu. Rev. Mater. Sci.* **1996**, *26*, 501.
(62) Sakurai, S.; Irie, H.; Umeda, H.; Nomura, S.; Lee, H. H.; Kim, J. K. *Macromolecules* **1998**, *31*, 336.
(63) Milner, S. T. *Macromolecules* **1994**, *27*, 2333.
(64) Pochan, D. J.; Gido, S. P.; Pispas, S.; Mays, J. W.; Ryan, A. J.; Fairclough, J. P. A.; Hamley, I. W.; Terrill, N. J. *Macromolecules* **1996**, *29*, 5091.
(65) Pochan, D. J.; Gido, S. P.; Pispas, S.; Mays, J. W. *Macromolecules* **1996**, *29*, 5099.
(66) Gido, S. P.; Lee, C.; Pochan, D. J.; Pispas, S.; Mays, J. W.; Hadjichristidis, N. *Macromolecules* **1996**, *29*, 7022.
(67) Lee, C.; Gido, S. P.; Pitsikalis, M.; Mays, J. W.; Tan, N. B.; Trevino, S. F.; Hadjichristidis, N. *Macromolecules* **1997**, *30*, 3732.
(68) Beyer, F. L.; Gido, S. P.; Buschl, C.; Iatrou, H.; Uhrig, D.; Mays, J. W.; Chang, M. Y.; Garetz, B. A.; Balsara, N. P.; Tan, N. B.; Hadjichristidis, N. *Macromolecules* **2000**, *33*, 2039.
(69) Lin, C. C.; Jonnalagadda, S. V.; Kesani, P. K.; Dai, H. J.; Balsara, N. P. *Macromolecules* **1994**, *27*, 7769.
(70) Gehlsen, M. D.; Bates, F. S. *Macromolecules* **1994**, *27*, 3611.
(71) Larson, R. G. *The Structure and Rheology of Complex Fluids*; Oxford University Press: Oxford, 1999; Chapter 13, pp 594−632.

MA034881G